Inorganic Chemistry

Article

pubs.acs.org/IC

Beyond Single-Wavelength SHG Measurements: Spectrally-Resolved SHG Studies of Tetraphosphonate Ester Coordination Polymers

Jan K. Zaręba,[†] Michał J. Białek,[§] Jan Janczak,[∥] Marcin Nyk,[†] Jerzy Zoń,[‡] and Marek Samoć*[,†]

[†]Advanced Materials Engineering and Modelling Group, Faculty of Chemistry and [‡]Department of Thermodynamics, Theory of Machines and Thermal Systems, Faculty of Mechanical and Power Engineering, Wrocław University of Technology, Wybrzeże Wyspiańskiego 27, 50-370 Wrocław, Poland

[§]Department of Chemistry, University of Wrocław, F. Joliot-Curie 14, 50-383 Wrocław, Poland

[∥]Institute of Low Temperature and Structural Research, Polish Academy of Sciences, Okólna 2, P.O. Box 1410, 50-950 Wrocław, Poland

Supporting Information

ABSTRACT: Powder second-harmonic generation (SHG) efficiencies are usually measured at single wavelengths. In the present work, we provide a proof of concept of spectrally resolved powder SHG measured for a newly obtained series of three non-centrosymmetric coordination polymers (CPs). CPs are constructed from tetrahedral linker—tetraphenylmethane-based tetraphosphonate octaethyl ester and cobalt(II) ions of mixed, octahedral (O_h), and tetrahedral (T_d), geometries and different sets of donors (CoO_6 vs CoX_3O). Isostructurality of the obtained materials allowed for the determination of anion-dependent tunability of SHG optical spectra and their relationship with solid-state absorption spectra.

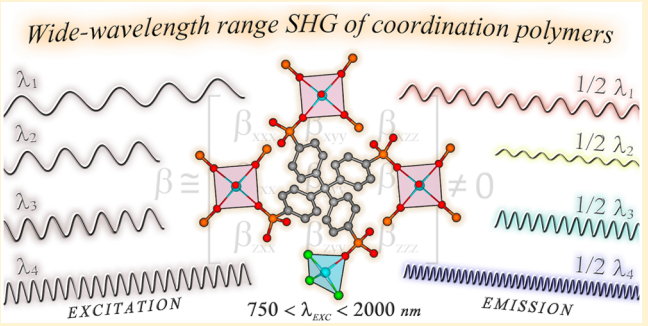

INTRODUCTION

Second-order optical nonlinearities of crystals are expressed by the nonlinear optical susceptibility tensor $\chi^{(2)}$ that can be accurately determined using the Maker fringe method. The technique is rather time-consuming and requires relatively large and good-quality single crystals. Some initial screening of new nonlinear materials may be, however, achieved by the powder second-harmonic generation (SHG) technique proposed in 1968 by Kurtz and Perry[1] and, independently, by Graja.[2] Despite some essential deficiencies,[3] this method still remains the most common technique for a rough estimation of SHG efficiency.

Second-order optical processes have already found many applications and therefore have been studied in a vast variety of materials, for example, inorganic[4] and organic[5] compounds, Langmuir—Blodgett films,[6] poled polymers,[7] quantum dots,[8] plasmonic nanostructures,[9] and, more recently, in coordination polymers (CPs).[10] Apart from materials for the most common uses such as that of frequency conversion in laser systems (SHG, optical parametric processes) and the electrooptic effect, materials for, for example, nonlinear optical microscopy or information storage are of much interest.[11]

Note that the lion's share of research in this field concerning new materials and using the powder SHG is done at several discrete excitation wavelengths being fundamental wavelengths of commonly employed lasers (e.g., Nd:YAG and Ti:sapphire at 1064 and 800 nm, respectively). The SHG efficiencies measured at a single wavelength are a fair description of material properties only if this wavelength is in the long wavelength region, far from any material resonances. Otherwise, similar to the case of third-order nonlinear optical phenomena (i.e., fs Z-scan measurements[12]), the nonlinear optical properties need to be determined in a sufficiently wide wavelength range to allow for deciding whether linear and/or nonlinear absorption and possible resonance enhancements influence the results and whether the determined properties have in any way a chance of being useful in an intended application.

While there are known techniques extending the simple Kurtz powder test, for example, temperature-resolved SHG (TR-SHG),[13] to the best of our knowledge, there have been reports on wide-wavelength range measurements of the second-harmonic response of inorganic materials[14] but none for coordination polymers (CPs). As a proof of concept, in this contribution we investigated spectrally resolved second-harmonic generation (SR-SHG) of a series of phosphonate ester CPs.

From the structural chemistry viewpoint, of increasing interest are coordination polymers based on phosphonic acids (polymeric metal phosphonates)[15] and phosphonic acid monoesters.[16] Phosphonate ester-derived CPs, however, remain a largely unexplored field,[17] especially when comparing with the overwhelming number of these materials based on carboxylic

Received: May 5, 2015
Published: October 22, 2015

DOI: 10.1021/acs.inorgchem.5b01939
Inorg. Chem. 2015, 54, 10568−10575

Table 1. Crystal and Structure Refinement Data

symbol of the structure	**1-Cl**	**1-Br**	**1-I**[a]
empirical formula	$C_{123}H_{168}Cl_{12}Co_6O_{40}P_{12}$[b]	$C_{123}H_{176}Br_{12}Co_6O_{40}P_{12}$	$C_{123}H_{176}I_{12}Co_6O_{40}P_{12}$[c]
M [g·mol^{-1}]	3437.19	3978.78	4542.67
crystal system	monoclinic	monoclinic	monoclinic
space group	$C2$ (No. 5)	$C2$ (No. 5)	$C2$ (No. 5)
a [Å]	20.790(3)	20.787(3)	21.142(5)
b [Å]	13.234(2)	13.323(2)	13.474(4)
c [Å]	30.305(3)	30.693(4)	30.950(7)
α, β, γ [deg]	90, 100.99(3), 90	90, 100.65(3), 90	90, 100.95(5), 90
V [Å^3]	8185(2)	8354(1)	8656(3)
Z	2	2	
density calculated [g·cm^{-3}]	1.395	1.582	
μ(Mo Kα) [mm^{-1}]	0.976	3.634	
F(000)	3544	3992	
crystal size [mm]	0.19 × 0.23 × 0.27	0.19 × 0.23 × 0.27	
temperature [K]	295(2)	295(2)	295(2)
radiation [Å]	Mo Kα 0.710 73	Mo Kα 0.710 73	Mo Kα 0.710 73
θ_{min}, θ_{max} [deg]	2.6, 28.0	2.9, 29.8	
hkl range	−24:27; −17:17; −39:39	−28:28; −16:18; −42:32	
reflections measured, independent	56 166, 19 584	51 473, 20 468	
R_{int}	0.069	0.065	
R_1, wR_2, S	0.0668, 0.1770, 1.02	0.0530, 0.0803, 1.01	
Flack parameter	0.04(2)	0.028(9)	
$\Delta\rho_{max}$, $\Delta\rho_{min}$ [e·Å^{-3}]	−0.44, 0.63	−0.79, 0.89	
CCDC No.	1061295	1061296	

[a]Data obtained during a measurement of cell parameters. [b]Water protons were not localized. [c]Proposed formula assuming isostructurality.

and N-donor ligands.[18] It should be also stressed that no nonlinear optical measurements have been conducted for any phosphonate ester-derived CP to date, while single-wavelength SHG experiments were reported for metal phosphonates,[19] also in the form of thin films.[20] The investigated CPs were constructed using a tetrahedral ligand based on tetraphenylmethane, namely, tetrakis[4-(diethoxyphosphoryl)phenyl]-methane (**1**, L), which was prepared according to recently published procedure.[21] Our three CPs (denoted as **1-Cl**, **1-Br**, and **1-I**) constitute an isostructural series, which additionally enabled the determination of counterion effect on SHG spectra.

EXPERIMENTAL SECTION

General Remarks. Ligand **1**, tetrakis[4-(diethoxyphosphoryl)-phenyl]methane, was prepared via nickel-catalyzed phosphonylation of tetrakis(4-bromophenyl)methane with triethyl phosphite. Other starting materials were of reagent grade purity and were obtained from commercial sources and used without further purification. Powder X-ray diffraction (PXRD) patterns of the coordination polymers were measured on a PANanalytical X'Pert diffractometer equipped with a Cu Kα radiation source (λ = 1.541 82 Å). Elemental analysis was performed using a CE Instruments CHNS 1110 elemental analyzer. Energy-dispersive X-ray (EDX) analysis was performed on coupled with scanning electron microscopy (SEM; microscope model JEOL JSM-6610LV) Oxford Aztec Energy detector at an acceleration voltage of 1.8 kV and a working distance of 10 mm. Thermogravimetric analysis (TGA) and differential thermal analysis (DTA) were conducted using a Setaram SETSYS 16/18 thermoanalyzer in the range of 20−800 °C at a heating rate of 5 °C/min in flowing nitrogen atmosphere. Mid-infrared (MIR) and far-infrared (FIR) spectra were obtained on a VERTEX 70 V FT-IR spectrometer (Bruker Optik GmbH, Ettlingen, Germany) in attenuated total reflection (ATR) measurement mode. Diffuse reflectance spectra (DRS) were obtained on a Cary 500 spectrophotometer in the range of 200−2000 nm using $BaCO_3$ as a reference. The absorption spectra were calculated from the Kubelka−Munk function: $F(R) = (1 - R)^2/2R = K/S$, where R is the diffuse reflectance, K is the molar absorption coefficient, and S is the scattering coefficient.

Synthesis. Synthesis of $[Co(H_2O)_2^{2+}]\cdot[CoCl_3^-]_2\cdot L_{1.5}$, (1-Cl). Ligand **1** (25.0 mg, 0.0289 mmol) was dissolved in 96% ethanol (1 mL) in a 10 mL glass vial. Then anhydrous $CoCl_2$ (7.5 mg, 0.0577 mmol) was added. Upon dissolution of cobalt(II) salt the solution turned light pink. Then on the top of the vial a screw cap was placed and lightly closed, to allow vapor diffusion. Next, the vial was transferred to a 100 mL chamber filled with diethyl ether (30 mL). Upon diffusion of diethyl ether the solution turned dark blue. After one week dark blue parallelepiped crystals appeared. Typical yield (with respect to the ligand): 22.3 mg (68%). The same product is also obtained when $CoCl_2\cdot 6H_2O$ is used. Anal. Calcd for $C_{123}H_{176}Cl_{12}Co_6O_{40}P_{12}$ (3445.21): C, 42.84; H, 5.15. Found: C, 42.89; H, 4.68 [%]. EDX analysis (molar ratio): Co/P/Cl, experimental 1:1.97:1.86, required: 1:2:2.

Synthesis of $[Co(H_2O)_2^{2+}]\cdot[CoBr_3^-]_2\cdot L_{1.5}$, (1-Br). Ligand **1** (25.0 mg, 0.0287 mmol) was dissolved in 96% ethanol (1 mL) in a 10 mL glass vial. Then anhydrous $CoBr_2$ (12.7 mg, 0.0580 mmol) was added. Upon dissolution of cobalt(II) salt the solution turned pink. Then on the top of the vial a screw cap was placed and lightly closed, to allow vapor diffusion. Next, the vial was transferred to a 100 mL chamber filled with diethyl ether (30 mL). Upon diffusion of diethyl ether the solution turned dark blue. After one week dark blue parallelepiped crystals appeared. Typical yield (with respect to the ligand): 23.5 mg (62%). Anal. Calcd for $C_{123}H_{176}Br_{12}Co_6O_{40}P_{12}$ (3978.78): C, 37.10; H, 4.46. Found: C, 36.90; H, 4.32 [%]. EDX analysis (molar ratio): Co/P/Br, experimental 1:1.96:1.89, required: 1:2:2. The same product is also obtained when $CoBr_2\cdot xH_2O$ is used.

Synthesis of $[Co(H_2O)_2^{2+}]\cdot[CoI_3^-]_2\cdot L_{1.5}$, (1-I). Ligand **1** (24.0 mg, 0.0277 mmol) was dissolved in 96% ethanol (1 mL) in a 10 mL glass vial. Then $CoI_2\cdot 6H_2O$ (23.3 mg, 0.056 mmol) was added. Upon dissolution of cobalt(II) salt the solution turned light orange. Then on the top of the vial a screw cap was placed and lightly closed, to allow vapor diffusion. Next, the vial was transferred to a 100 mL chamber filled with diethyl ether. Upon diffusion of diethyl ether the solution turned dark green. After two weeks dark green parallelepiped crystals appeared. Typical yield (with respect to the ligand): 24.2 mg (58%).

DOI: 10.1021/acs.inorgchem.5b01939
Inorg. Chem. 2015, 54, 10568−10575

Anal. Calcd for $C_{123}H_{176}I_{12}Co_6O_{40}P_{12}$ (4542.67): C, 32.49; H, 3.91. Found: C, 32.20; H, 3.66 [%]. EDX analysis (molar ratio): Co/P/I, experimental 1:2.04:1.92, required: 1:2:2. MIR and FIR spectra are presented in Figures S1 and S2, Supporting Information, respectively. IR tentative assignments are given in Table S1, Supporting Information. Note that electron beam caused decomposition of samples **1-Cl**, **1-Br**, and **1-I**, which can be concluded from decreasing percentage amount of halogens in several subsequent measurements. The Co/P ratio for all samples remained constant.

X-ray Crystallography. All the obtained single crystals were used for data collection on a four-circle KUMA KM4 diffractometer equipped with a two-dimensional CCD area detector. Graphite monochromatized Mo Kα radiation (λ = 0.710 73 Å) and the ω-scan technique ($\Delta\omega$ = 1°) were applied, while additional data collection and reduction, along with absorption correction, were performed using the CrysAlis software package.[22] The structures were solved by direct methods using SHELXS-97,[23] revealing the positions of all or almost all non-hydrogen atoms. The remaining atoms were located as a result of subsequent difference Fourier syntheses. The structures were refined using SHELXL-97[23] with anisotropic displacement parameters. Hydrogen atoms connected to carbon atoms were constrained as a riding model. The positions of the H atoms of water molecules were located on a difference Fourier map, where possible, and constrained. The collection parameters data, crystallographic data, and final agreement parameters are listed in Table 1.

Selected geometrical parameters can be found in Tables S2–S5, Supporting Information. The geometry parameters of hydrogen bonds are listed in Tables S6 and S7, Supporting Information. Visualization of the structures was conducted using the Diamond program,[24] while a topological simplification of coordination networks was performed with the ToposPro package.[25] Geometrical features of intermolecular interactions were determined with the help of Platon software.[26]

Note that only crystal structures **1-Cl** and **1-Br** were determined from single crystals. Despite numerous trials we were not able to obtain single crystals of **1-I** of satisfactory X-ray quality. Presented cell parameters of **1-I** were determined in preliminary measurement. Isostructurality of **1-I** was confirmed by PXRD data (Figure S3, Supporting Information).

Wide-Wavelength Range Second-Harmonic Generation Measurements. The experimental routine was as follows. Prior to measurements, crystalline powders of coordination polymers were sieved through a mini-sieve set (Aldrich) to the following sizes: below 63, 63–88, 88–125, 125–177, and 177–250 μm. For wide-wavelength range SHG measurements powdered samples of the non-centrosymmetric coordination polymers (**1-Cl**, **1-Br**, **1-I**) and that of KH_2PO_4 (KDP) with the same particle size (125–177 μm), which was used as a reference material, were mounted between separate microscope glass slides and excited by tunable femtosecond laser pulses from the laser system consisting of a Quantronix Integra-C regenerative amplifier operating as an 800 nm pump and a Quantronix-Palitra-FS BIBO crystal-based optical parametric amplifier. This system delivers wavelength-tunable pulses of ~130 fs length and was operated at the repetition rate of 1 kHz. The incident beam was directed to the plane of sample at ~45°, while the detector was placed in front of the sample. Such a geometry precluded from collection most of the reflected exciting beam. Laser beam intensity was attenuated by a Glan laser polarizer, and spectra of the SHG emission were recorded by an Ocean Optics 2000 fiber-coupled CCD spectrograph for excitation wavelengths of 750–1700 nm and Ocean Optics NIRQuest512–2.2 for excitation wavelengths of 1800–2000 nm. The geometry of the experimental setup and intensity of the laser beam were exactly the same for all samples at a given wavelength. Unwanted wavelengths that are usually present in the output of an optical parametric amplifier were removed using color glass filters. After setting the output wavelength (750–2000 nm, ~25 nm step), the intensity of the beam was attenuated, when needed, by using polarizing optics, to avoid sample decomposition. Such a precaution was especially needed for wavelengths shorter than 1000 nm. Measurements were regarded as reliable when emitted signals did not noticeably change over the course of laser exposure for three consecutive scans. A different integrating time was used for coordination polymers (typically 10 000–30 000 ms) and for the KDP sample (1000–10 000 ms) to ensure a reliable signal-to-noise ratio. The intensity of the signal was normalized to the same time of collection. ***Caution!*** *Work with the high-power laser brings danger to the eyes, especially in spectral range in which the beam is invisible. Adequate eye protection should be used during measurements.*

RESULTS AND DISCUSSION

Synthesis and Structure. Single crystals of coordination polymers were obtained via vapor diffusion of ethanol solutions of compound **1** and cobalt(II) halides with diethyl ether (Scheme 1). Crystal structures were determined for **1-Cl** and **1-Br** (Table 1).

Scheme 1. Structural Formula and Route to Preparation of the Coordination Polymers from 1 and Cobalt(II) Halide Salts (chloride, bromide, iodide)

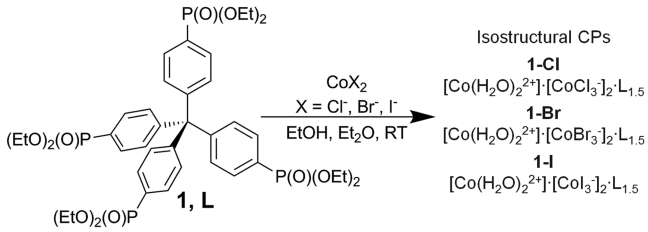

Phase purity and isostructurality of samples **1-Cl**, **1-Br**, **1-I** were proven by PXRD measurements on bulk samples. The change of the halide from lighter to a heavier one increases the relative intensity of reflections from $(11\bar{2})$ and $(20\bar{2})$ crystallographic planes at 2θ = 9.5°, which stands in agreement with theoretical powder patterns (Figure S3, Supporting Information).

Coordination polymers crystallize in a non-centrosymmetric space group *C*2. Their stoichiometry, derived from asymmetric units (Figure S4, Supporting Information), can be represented with formula $[Co(H_2O)_2^{2+}]\cdot[CoX_3^-]_2\cdot L_{1.5}$, where X = halide anion and L = $C[C_6H_4P(O)(OC_2H_5)_2]_4$.

Two crystallographically independent molecules of ligand **1** are bound to cobalt(II) centers through phosphoryl oxygen atoms. One molecule (L1Co) is coordinated by three octahedral CoO_6 units and one tetrahedral CoX_3 unit, while the other (L2Co) is coordinated by two CoO_6 and two CoX_3. The presence of one $[CoO_6]^{2+}$ and two independent $[CoX_3]^-$ ions assures charge balance. The octahedral coordination unit includes an equatorial set of phosphoryl donors with two axial positions occupied by water molecules. Co–O bond distances are in a range typical for neutral oxygen donors (2.07–2.12 Å, Tables S2 and S4, Supporting Information). In the tetrahedral units the Co^{2+} ion is surrounded by three halide anions and one phosphoryl oxygen.

Note that compounds possessing simultaneously tetrahedral and octahedral cobalt(II) centers are rather unexplored.[27] Reports concerning such systems were predominantly concentrated on elucidation of their magnetic behavior due to complicated character of magnetic exchange between cobalt(II) ions.[28]

A coordination network of **1-X** is two-dimensional (Figure 1) with (001) layers composed of L1Co and L2Co in a 2:1 ratio. Adjacent layers, translated by the *c* distance, interact mostly through water O–H···X hydrogen bonds and dispersion forces.

DOI: 10.1021/acs.inorgchem.5b01939
Inorg. Chem. 2015, 54, 10568–10575

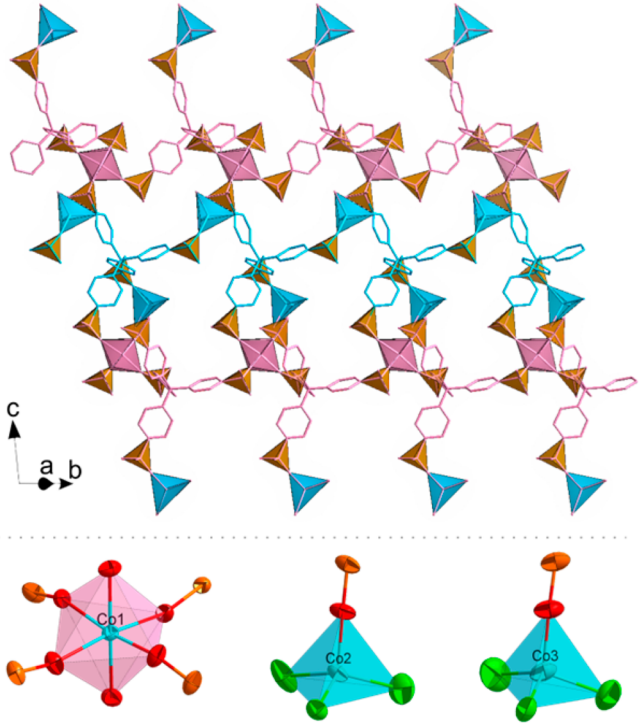

Figure 1. Isolated layer of **1-Cl**. Phosphonate groups shown as orange tetrahedra, CoO_6 octahedra and L1Co molecules marked pink, and $CoCl_3O$ and L2Co moieties marked blue. One can see pink CoO_6 surrounded by four orange tetrahedra and blue $CoCl_3O$ with one attached. The lower part of the figure shows independent coordination polyhedra present in the structure. Displacement ellipsoids are drawn with 30% probability.

Topological simplification[25] of the **1-X** networks leads to a two-periodic two-nodal net, featured by the $(6^3{\cdot}6^6)$ net point symbol, where (6^3) and (6^6) indices match a three-connected ligand node (L1Co) and a four-connected Co node (CoO_6), respectively (Figure 2). From Figure 2a one can clearly see close intermolecular contacts of halide and water ligands that unite all layers into the three-dimensional structure. This particular motif brings two tetrahedral and one octahedral cobalt(II) centers together. In this motif, one CoX_3 comes, as mentioned, from the adjacent layer, and the other one originates from a twofold symmetry-related L1Co molecule in the same layer (Figure 3).

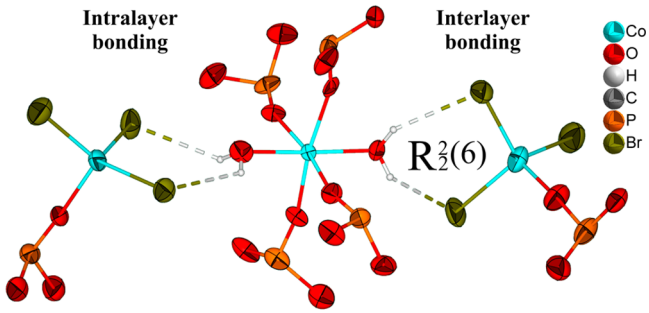

Figure 3. Hydrogen bond motifs around CoO_6 in **1-Br**. O···X distances are equal from 3.25 to 3.37 Å (from 3.06 to 3.16 Å in **1-Cl**).

Wide-Wavelength Second-Harmonic Generation Measurements and Phase-Matching Study. Since powder SHG is particle size-dependent, to ensure comparability of measurements the samples of CPs and KDP (used herein as reference) were mechanically ground and sieved to following sizes: below 63, 63−88, 88−125, 125−177, and 177−250 μm. Wide-wavelength SHG measurements were conducted at samples of 125−177 μm size in the range from 750 to 2000 nm with 25 nm step using a tunable femtosecond laser as excitation source. Note that our instruments used for collection of emitted radiation allowed for detection of SHG signal in the ranges of 350−850 and above 900 nm, which resulted in a gap in the results for excitation wavelengths between 1700 and 1800 nm. The emitted second harmonic was collected in backscattering mode (see Experimental Section). The obtained spectrally resolved SHG results for CPs **1-Cl**, **1-Br**, and **1-I** are presented in Figure 4.

In general, in the whole spectral range the obtained SHG intensities of the investigated CPs do not exceed 0.1 of that of

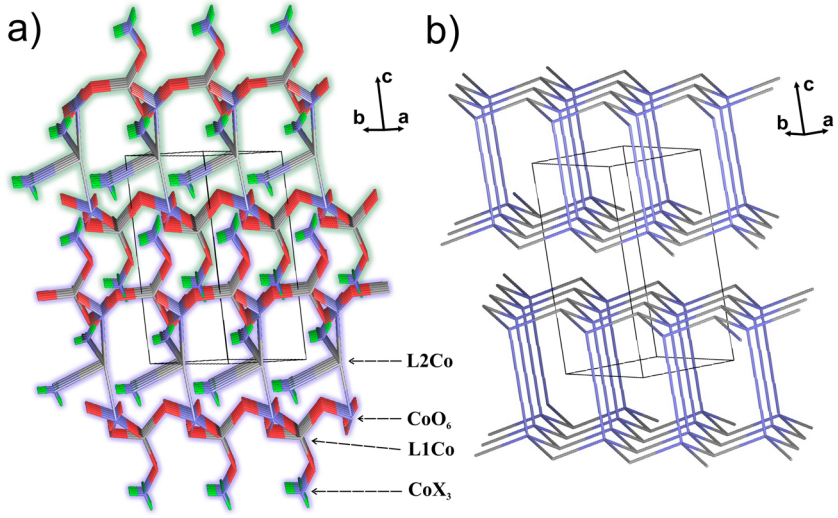

Figure 2. (a) Point-and-stick topological presentations of two adjacent layers of **1-Cl**, one highlighted blue and the other green. Atoms and organic cores simplified to points. Co−blue, ligands' cores−gray, Cl−green, O−red; (b) Topology of two adjacent layers after zero-, one-, and two-connected nodes removal. The net is composed of a three-connected ligand node (L1Co) and a four-connected octahedral Co node (CoO_6).

DOI: 10.1021/acs.inorgchem.5b01939
Inorg. Chem. 2015, 54, 10568−10575

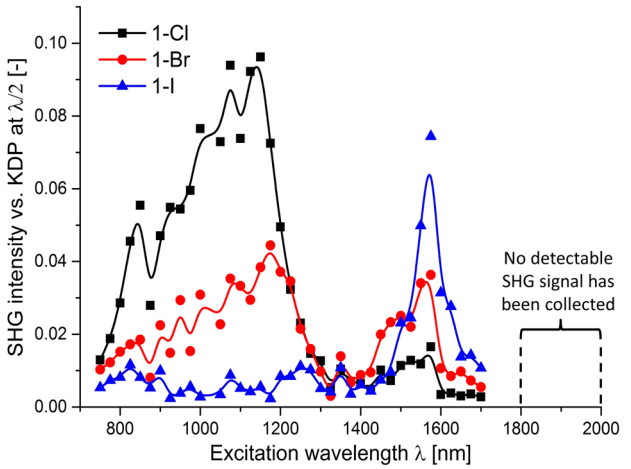

Figure 4. Plots (**1-Cl** – black, **1-Br** – red, **1-I** – blue) of normalized SHG intensity collected at $\lambda/2$ in the function of excitation wavelength λ. Lines are just to guide the eyes.

KDP. Our attention, however, was directed toward interesting anion-tunability of the SHG response: in the range of 750–1300 nm the strongest signal is obtained from **1-Cl** (peaking at 1150 nm, 0.096); that of **1-Br** is weaker (1175 nm, 0.044), while the iodide-derived CP **1-I** is significantly less efficient (1250 nm, 0.011). When moving to longer wavelengths **1-Br** has the biggest values between 1300 and 1500 nm (up to 0.025 of KDP), and finally, the SHG response is most pronounced at 1575 nm for **1-I** (up to 0.074 of KDP). Interestingly, SHG response of **1-Br** and **1-Cl** is lower at this wavelength (0.036 and 0.016 of KDP, respectively) creating a reverse trend (**1-I** > **1-Br** > **1-Cl**) in comparison to SHG intensities collected at 1150 nm.

From 1575 to 1700 nm all SHG intensities gradually decrease. Although no data are available for excitation wavelengths in the range from 1700 to 1800 nm we expect that the SHG response does not exceed 0.01 that of KDP. This is supported by the fact that excitation in the range of 1800–2000 nm resulted in no detectable SHG signal, suggesting overall little response in FIR region.

It should be stressed that change of only the counterion has dramatic influence on both the position of maxima and the relative intensity of SHG, which is most striking when comparing **1-Cl** and **1-I**.

As there are no papers on SHG properties of phosphonate ester CPs we cannot make direct comparisons of obtained relative SHG intensities with any member of the same class. However, single-wavelength SHG experiments were conducted for CPs based on various phosphonic acids. There are two reports of phosphonic coordination compounds with cobalt(II). Yang et al. recently reported efficiency equal to 0.6 urea (which corresponds to 15 times of KDP) in cobalt(II) phosphonocarboxylate, but unfortunately, few measurement details have been provided.[19e] The origin of quite high SHG response has not been explained. On the contrary, Zhou et al. described cobalt(II) phosphonocarboxylate that showed no detectable SHG activity for fundamental wavelength of 1064 nm (Zn analogue has efficiency equal to 0.2 of KDP). The absence of the SHG signal was ascribed to self-absorption of emitted radiation by the colored compound and to the racemic twinning of enantiomeric crystals.[19d] It is also worth mentioning that free phosphonic acids were also the subject of SHG characterization, and their efficiencies were in the range from 0.1 to 0.6 that of urea at 1054 nm (~2.5 to 15 of KDP).[29]

Once the spectra of SHG response for **1-Cl**, **1-Br**, and **1-I** were identified we selected two maxima for which a possibility of phase-matching was investigated (1150 and 1575 nm). As shown in Figure 5 there is no visible increasing trend of the SHG response with the size of particles, which indicates the lack of type-I phase matching.

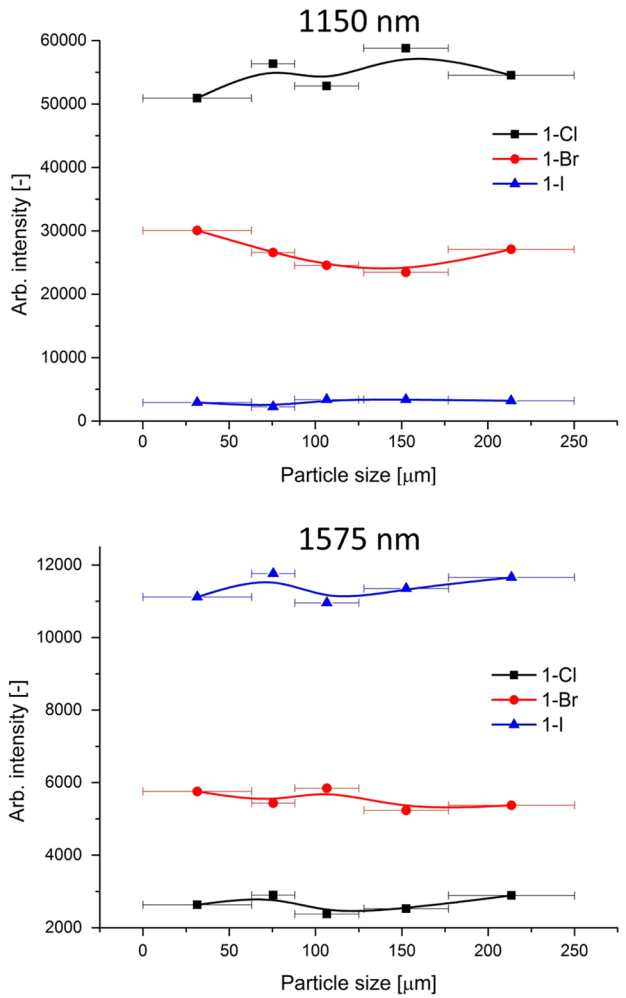

Figure 5. Plots of SHG counts vs particle size for 1150 and 1575 nm wavelength excitation. Lines are just to guide the eyes.

Rationalization of Wide-Wavelength Second-Harmonic Generation Spectra. Overall, the obtained SHG spectra are quite complex, and for this reason, we considered three possible factors that may have influence on obtained dependencies: the hyperpolarizability of halogen ions, their electronegativity, and self-absorption of incident and emitted radiation.

Hyperpolarizability of the halogen counterions themselves probably has only a minor impact on the SHG spectra as the intensity of this process in a significant part of the spectrum is in fact the lowest for iodide, the anion with the biggest ionic radius, and thus the biggest polarizability. In fact, the spectral changes of the signal intensity are better related to increase of electronegativity in the order of I < Br < Cl. Increase of electronegativity may indeed modify charge transfer between complex anion CoX_3^- (X = Cl, Br, I) and the diethoxyphos-

DOI: 10.1021/acs.inorgchem.5b01939
Inorg. Chem. 2015, 54, 10568–10575

phoryl group attached to the aromatic core, leading to the enhanced second harmonic response.

One can suspect that it is the extent of absorption of incident and emitted radiation that determines where SHG will be suppressed. Thus, this prompted us to investigate solid-state absorption spectra of the obtained materials and to relate them with the SHG spectra.

The halide ions are coordinated to the tetrahedral cobalt(II) ion and directly influence its chromophoric environment. Substitution of halogen from lighter **1-Cl** to heavier **1-I** results in red shifting of both strong absorptions bands resulting from Laporte-allowed d−d $^4A_2 \rightarrow {}^4T_1(P)$ (∼650 nm) and $^4A_2 \rightarrow {}^4T_1(F)$ transitions (∼1555 nm) within the tetrahedral cobalt-(II) ions (Figure S5, Supporting Information. All assignments of transitions are collected in Table S8, Supporting Information). Interestingly, in the case of **1-I** the absorption spectrum reveals an additional band centered at 387 nm, which is not present in the other two isomorphs. The reason for its presence is not entirely clear, but considering its intensity, we suppose it may be a charge-transfer (CT) transition involving iodide anions.

It is worth mentioning that counterion dependence of SHG was previously studied in CPs based on chiral octupolar organoboron ligands, yet intensities of SHG excited at 1064 nm were found to increase in reverse order (Cl < Br < I).[30] However, the anions present there were not connected via coordination bonds to the metal center but were residing uncoordinated in the crystal lattice. Presented herein CPs are structurally different, as halide ions are coordinated to the tetrahedral cobalt centers and thus directly influencing their crystal field. This fact results in the shifting the position of the d−d transitions maxima—thus having significant impact on the absorption spectra and consequently, on SHG spectra.

We found the most efficient SHG in a range of wavelengths at which the exciting (fundamental) and emitted waves may be only weakly absorbed. Extent of absorption of the fundamental wave is determined by absorption spectrum of the sample, but one must also take into account self-absorption of the emitted second harmonic. Consequently, capability of material to self-absorb SHG is visualized by plotting the absorption spectrum against twice the wavelength. By consideration of both of these absorption spectra as an overlay one can determine "optical windows" of lower absorption of the material. Figure 6 shows solid-state absorption spectra plotted against one and two times the wavelength. For **1-Cl** and **1-Br** the main "optical window" can be found from 750 to 1200 nm, which stays in agreement with maximum of SHG intensity found for these CPs (Figure 4). For **1-I** in this region much bigger self-absorption is observed, and therefore the obtained SHG efficiency is respectively lower. The presence of a second region, in which local maximum of SHG emission takes place (∼1575 nm) is not so straightforward to explain on the basis of absorption spectra as it lies in the region of increasing absorption (plotted vs once the wavelength) and, simultaneously, of decreasing absorption (plotted vs twice the wavelength). Notice that comparisons of SHG spectra and absorption spectra should be treated rather qualitatively and therefore can show only general trends.

The modest powder SHG response of the three coordination polymers, apart from the presence of broad and strong absorption bands, may be attributed to the lack of a suitable donor−acceptor system, which would be responsible for large transition moment and large excited-state dipole moment,

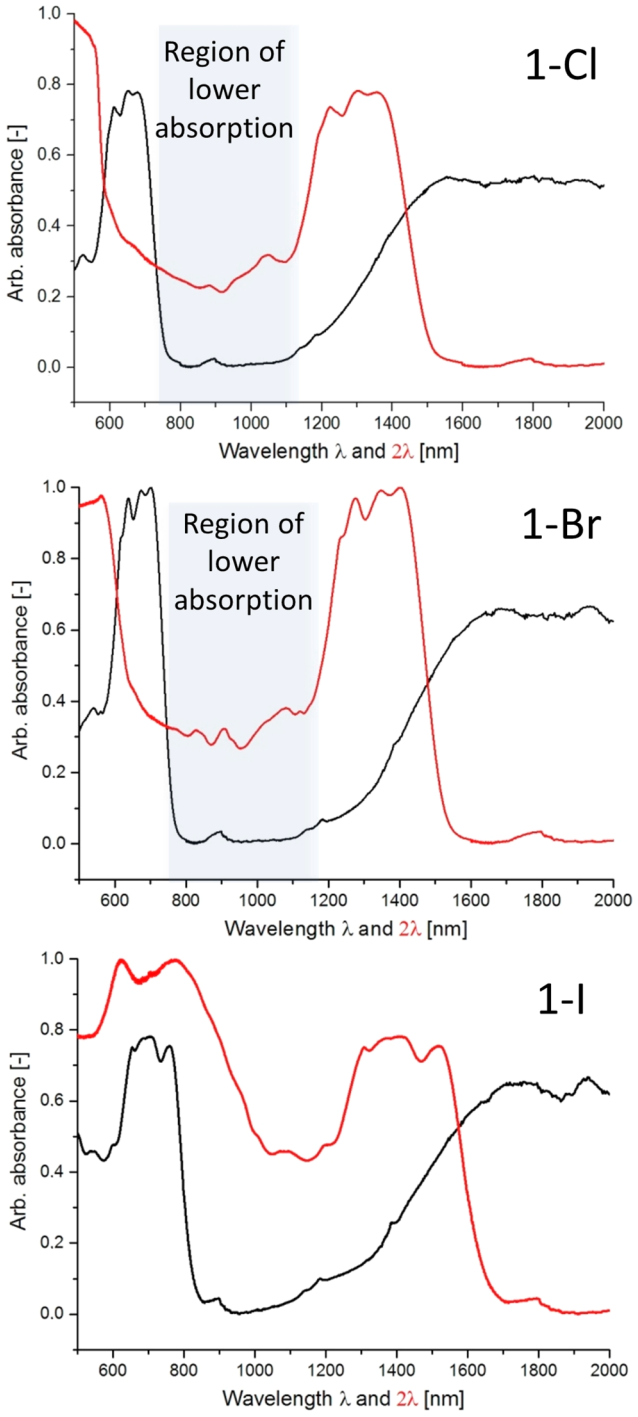

Figure 6. Overlays of the solid-state absorption spectra plotted against one and two times the wavelength (black and red lines, respectively) for **1-Cl**, **1-Br**, **1-I**. For the spectra of **1-Cl** and **1-Br** regions of optical transmission windows are indicated with gray rectangles.

which are essential for efficiency of second-order optical phenomena. The ligand used here has S_4 symmetry and, as octupolar molecule, has nonvanishing first hyperpolarizability. However, according to our preliminary calculations at B3LYP 6-311++G(d,p) level of theory (see the Supporting Information), the total static hyperpolarizability β of ligand **1**, despite quite a large aromatic moiety, is ∼5 times lower than that for urea (1.4×10^{-31} and 7.7×10^{-31} esu, respectively) which rationalizes the obtained experimental results.

DOI: 10.1021/acs.inorgchem.5b01939
Inorg. Chem. 2015, 54, 10568−10575

Thermogravimetric Analysis. Scarce reports of phosphonate ester coordination polymers prompted us to explore thermogravimetric properties of our samples. Thermal decomposition of the isostructural CPs takes place in three steps (Figure 7) occurring at the same temperature. The first

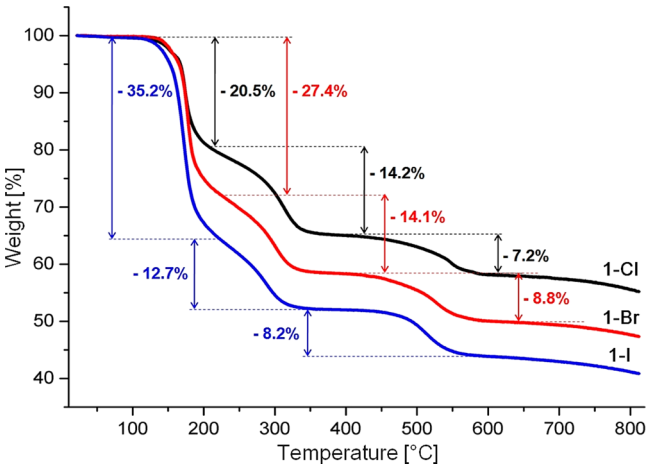

Figure 7. TGA plots of coordination polymers **1-Cl**, **1-Br**, **1-I**.

step, beginning at 115−120 °C, is mainly attributed to the dissociation of halogen atoms connected to the tetrahedral cobalt center and to the loss of coordination water, as also confirmed by two endothermic peaks in DTA (Figure S6, Supporting Information). The next step, which is not well-separated from the previous one, involves dissociation of ethyl groups (ca. 230 °C), while the drop of mass at ∼440 °C can be attributed to partial dephosphonylation of the ligand molecule. For comparison, TGA of ligand **1** (Figure S7, Supporting Information) shows the first stage of noticeable mass loss at higher temperature (260 °C). Thus, it can be concluded that thermal stability of the CPs is limited by the presence of CoX_3^- anions and coordination water rather than the strength of neutral phosphoryl oxygen atom coordination.

CONCLUSIONS

In conclusion, we provided the proof of concept of spectrally resolved Kurtz−Perry powder tests on polycrystalline phosphonate ester coordination polymers as a method that provides more information than that available from single-wavelength measurements, particularly in the cases in which absorption of the samples may be an important factor. Isomorphous CPs showed possibility of anion-tunable influence on the SHG spectra; in particular, the change of the counterion can significantly modify the maximum SHG efficiency. The dispersion of that efficiency can be qualitatively rationalized, by comparison with the solid-state absorption spectra.

Moreover, from the structural point of view, we have presented and characterized new members of an intriguing class of phosphonate ester coordination polymers built on the tetrahedral ligand core, in which cobalt(II) centers are both octahedral and tetrahedral.

ASSOCIATED CONTENT

Supporting Information

The Supporting Information is available free of charge on the ACS Publications website at DOI: 10.1021/acs.inorgchem.5b01939.

IR (MIR, FIR) spectra and assignments, crystallographic data, PXRD, DRS, additional thermogravimetric data, and static hyperpolarizability DFT calculations of the ligand. (PDF)

X-ray crystallographic data for **1-Cl** and **1-Br**. (CIF)

AUTHOR INFORMATION

Corresponding Author

*E-mail: marek.samoc@pwr.edu.pl.

Author Contributions

All authors have given approval to the final version of the manuscript.

Notes

The authors declare no competing financial interest.

ACKNOWLEDGMENTS

We acknowledge with thanks statutory activity subsidy from the Polish Ministry of Science and Higher Education for the Faculty of Chemistry, Wrocław Univ. of Technology, Wrocław, Poland. J.K.Z., M.N., and M.S. acknowledge financial support from the Polish National Science Centre Maestro Grant No. DEC-2013/10/A/ST4/00114. We also gratefully acknowledge the instrumental Grant No. 6221/IA/119/2012 from the Polish Ministry of Science and Higher Education, which supported our Integrated Laboratory of Research and Engineering of Advanced Materials where IR and EDX measurements were performed. A grant of computer time from the Wroclaw Center for Networking and Supercomputing is gratefully acknowledged.

REFERENCES

(1) Kurtz, S. K.; Perry, T. T. *J. Appl. Phys.* **1968**, *39*, 3798−3813.
(2) Graja, A. *Phys. Status Solidi B* **1968**, *27*, K93−K97.
(3) Aramburu, I.; Ortega, J.; Folcia, C. L.; Etxebarria, J. *Appl. Phys. B: Lasers Opt.* **2014**, *116*, 211−233.
(4) (a) Becker, P. *Adv. Mater.* **1998**, *10*, 979−992. (b) Abudourehe-man, M.; Wang, L.; Zhang, X.; Yu, H.; Yang, Z.; Lei, C.; Han, J.; Pan, S. *Inorg. Chem.* **2015**, *54*, 4138−4142.
(5) (a) Cariati, E.; Botta, C.; Danelli, S. G.; Forni, A.; Giaretta, A.; Giovanella, U.; Lucenti, E.; Marinotto, D.; Righetto, S.; Ugo, R. *Chem. Commun.* **2014**, *50*, 14225−14228. (b) Simon, F.; Clevers, S.; Gbabode, G.; Couvrat, N.; Agasse-Peulon, V.; Sanselme, M.; Dupray, V.; Coquerel, G. *Cryst. Growth Des.* **2015**, *15*, 946−960. (c) Coluccini, C.; Caricato, M.; Cariati, E.; Righetto, S.; Forni, A.; Pasini, D. *RSC Adv.* **2015**, *5*, 21495−21503.
(6) Ashwell, G. J. *J. Mater. Chem.* **1999**, *9*, 1991−2003.
(7) (a) Robinson, B. H.; Dalton, L. R.; Harper, A. W.; Ren, A.; Wang, F.; Zhang, C.; Todorova, G.; Lee, M.; Aniszfeld, R.; Garner, S.; Chen, A.; Steier, W. H.; Houbrecht, S.; Persoons, A.; Ledoux, I.; Zyss, J.; Jen, A. K. Y. *Chem. Phys.* **1999**, *245*, 35−50. (b) van der Boom, M. E. *Angew. Chem., Int. Ed.* **2002**, *41*, 3363−3366.
(8) (a) Zielinski, M.; Oron, D.; Chauvat, D.; Zyss, J. *Small* **2009**, *5*, 2835−2840. (b) Liu, X.; Zhang, Q.; Chong, W. K.; Yip, J. N.; Wen, X.; Li, Z.; Wei, F.; Yu, G.; Xiong, Q.; Sum, T. C. *ACS Nano* **2015**, *9*, 5018−5026.
(9) (a) Salomon, A.; Zielinski, M.; Kolkowski, R.; Zyss, J.; Prior, Y. *J. Phys. Chem. C* **2013**, *117*, 22377−22382. (b) Kolkowski, R.; Szeszko, J.; Dwir, B.; Kapon, E.; Zyss, J. *Opt. Express* **2014**, *22*, 30592−30606.
(10) (a) Evans, O. R.; Xiong, R. G.; Wang, Z.; Wong, G. K.; Lin, W. *Angew. Chem., Int. Ed.* **1999**, *38*, 536−538. (b) Evans, O. R.; Lin, W. *Acc. Chem. Res.* **2002**, *35*, 511−522. (c) Wang, C.; Zhang, T.; Lin, W. *Chem. Rev.* **2012**, *112*, 1084−1104.
(11) (a) Campagnola, P. J.; Loew, L. M. *Nat. Biotechnol.* **2003**, *21*, 1356−1360. (b) Reeve, J. E.; Collins, H. A.; De Mey, K.; Kohl, M. M.; Thorley, K. J.; Paulsen, O.; Clays, K.; Anderson, H. L. *J. Am. Chem.*

DOI: 10.1021/acs.inorgchem.5b01939
Inorg. Chem. 2015, 54, 10568−10575

Soc. **2009**, *131*, 2758−2759. (c) Demeritte, T.; Fan, Z.; Sinha, S. S.; Duan, J.; Pachter, R.; Ray, P. C. *Chem. - Eur. J.* **2014**, *20*, 1017−1022.
(12) Szeremeta, J.; Nyk, M.; Wawrzynczyk, D.; Samoć, M. *Nanoscale* **2013**, *5*, 2388−2393.
(13) (a) Clevers, S.; Rougeot, C.; Simon, F.; Sanselme, M.; Dupray, V.; Coquerel, G. *J. Mol. Struct.* **2014**, *1078*, 61−67. (b) Wu, X.; Park, H.; Zhu, X. Y. *J. Phys. Chem. C* **2014**, *118*, 10670−10676. (c) Ji, C.; Sun, Z.; Zhang, S.; Zhao, S.; Chen, T.; Tang, Y.; Luo, J. *Chem. Commun.* **2015**, *51*, 2298−2300. (d) Simon, F.; Clevers, S.; Gbabode, G.; Couvrat, N.; Agasse-Peulon, V.; Sanselme, M.; Dupray, V.; Coquerel, G. *Cryst. Growth Des.* **2015**, *15*, 946−960.
(14) (a) Banerjee, S.; Malliakas, C. D.; Jang, J. I.; Ketterson, J. B.; Kanatzidis, M. G. *J. Am. Chem. Soc.* **2008**, *130*, 12270−12272. (b) Bera, T. K.; Jang, J. I.; Ketterson, J. B.; Kanatzidis, M. G. *J. Am. Chem. Soc.* **2009**, *131*, 75−77. (c) Haynes, A. S.; Saouma, F. O.; Otieno, C. O.; Clark, D. J.; Shoemaker, D. P.; Jang, J. I.; Kanatzidis, M. G. *Chem. Mater.* **2015**, *27*, 1837−1846. (d) Syrigos, J. C.; Clark, D. J.; Saouma, F. O.; Clarke, S. M.; Fang, L.; Jang, J. I.; Kanatzidis, M. G. *Chem. Mater.* **2015**, *27*, 255−265.
(15) (a) Shimizu, G. K. H.; Vaidhyanathan, R.; Taylor, J. M. *Chem. Soc. Rev.* **2009**, *38*, 1430−1449. (b) Gagnon, K. J.; Perry, H. P.; Clearfield, A. *Chem. Rev.* **2012**, *112*, 1034−1054. (c) Białek, M. J.; Janczak, J.; Zoń, J. *CrystEngComm* **2013**, *15*, 390−399. (d) Kinnibrugh, T. L.; Ayi, A. A.; Bakhmutov, V. I.; Zoń, J.; Clearfield, A. *Cryst. Growth Des.* **2013**, *13*, 2973−2981. (e) Bazaga-Garcia, M.; Colodrero, R. M. P.; Papadaki, M.; Garczarek, P.; Zoń, J.; Olivera-Pastor, P.; Losilla, E. R.; Leon-Reina, L.; Aranda, M. A. G.; Choquesillo-Lazarte, D.; Demadis, K. D.; Cabeza, A. *J. Am. Chem. Soc.* **2014**, *136*, 5731−5739. (f) Ramaswamy, P.; Wong, N. E.; Gelfand, B. S.; Shimizu, G. K. H. *J. Am. Chem. Soc.* **2015**, *137*, 7640−7643.
(16) (a) Iremonger, S. S.; Liang, J.; Vaidhyanathan, R.; Martens, I.; Shimizu, G. K. H.; Daff, T. D.; Aghaji, M. Z.; Yeganegi, S.; Woo, T. K. *J. Am. Chem. Soc.* **2011**, *133*, 20048−20051. (b) Iremonger, S. S.; Liang, J.; Vaidhyanathan, R.; Shimizu, G. K. H. *Chem. Commun.* **2011**, *47*, 4430−4432. (c) Taylor, J. M.; Vaidhyanathan, R.; Iremonger, S. S.; Shimizu, G. K. H. *J. Am. Chem. Soc.* **2012**, *134*, 14338−14340. (d) Gelfand, B. S.; Lin, J. B.; Shimizu, G. K. H. *Inorg. Chem.* **2015**, *54*, 1185−1187.
(17) (a) Maxim, C.; Matni, A.; Geoffroy, M.; Andruh, M.; Hearns, N. G. R.; Clerac, R.; Avarvari, N. *New J. Chem.* **2010**, *34*, 2319−2327. (b) Hu, X.; Dou, W.; Xu, C.; Tang, X.; Zheng, J.; Liu, W. *Dalton Trans.* **2011**, *40*, 3412−3418. (c) Zubatyuk, R. I.; Sinelshchikova, A. A.; Enakieva, Y. Y.; Gorbunova, Y. G.; Tsivadze, A. Y.; Nefedov, S. E.; Bessmertnykh-Lemeune, A.; Guilard, R.; Shishkin, O. V. *CrystEngComm* **2014**, *16*, 10428−10438.
(18) (a) Yaghi, O. M.; Li, G.; Li, H. *Nature* **1995**, *378*, 703−706. (b) Kim, J.; Chen, B. L.; Reineke, T. M.; Li, H. L.; Eddaoudi, M.; Moler, D. B.; O'Keeffe, M.; Yaghi, O. M. *J. Am. Chem. Soc.* **2001**, *123*, 8239−8247. (c) Yaghi, O. M.; O'Keeffe, M.; Ockwig, N. W.; Chae, H. K.; Eddaoudi, M.; Kim, J. *Nature* **2003**, *423*, 705−714. (d) Park, K. S.; Ni, Z.; Cote, A. P.; Choi, J. Y.; Huang, R.; Uribe-Romo, F. J.; Chae, H. K.; O'Keeffe, M.; Yaghi, O. M. *Proc. Natl. Acad. Sci. U. S. A.* **2006**, *103*, 10186−10191. (e) Farha, O. K.; Hupp, J. T. *Acc. Chem. Res.* **2010**, *43*, 1166−1175. (f) Furukawa, H.; Cordova, K. E.; O'Keeffe, M.; Yaghi, O. M. *Science* **2013**, *341*, 974−986.
(19) (a) Liu, X.-G.; Zhou, K.; Dong, J.; Zhu, C.-J.; Bao, S.-S.; Zheng, L.-M. *Inorg. Chem.* **2009**, *48*, 1901−1905. (b) Liu, X. G.; Huang, J.; Bao, S. S.; Li, Y. Z.; Zheng, L. M. *Dalton Trans.* **2009**, 9837−9842. (c) Li, J. T.; Cao, D. K.; Akutagawa, T.; Zheng, L. M. *Dalton Trans.* **2010**, *39*, 8606−8608. (d) Zhou, T.-H.; He, Z.-Z.; Xu, X.; Qian, X.-Y.; Mao, J.-G. *Cryst. Growth Des.* **2013**, *13*, 838−843. (e) Yang, X.-J.; Bao, S.-S.; Ren, M.; Hoshino, N.; Akutagawa, T.; Zheng, L.-M. *Chem. Commun.* **2014**, *50*, 3979−3981.
(20) (a) Katz, H. E.; Scheller, G.; Putvinski, T. M.; Schilling, M. L.; Wilson, W. L.; Chidsey, C. E. D. *Science* **1991**, *254*, 1485−1487. (b) Neff, G. A.; Helfrich, M. R.; Clifton, M. C.; Page, C. J. *Chem. Mater.* **2000**, *12*, 2363−2371. (c) Morotti, T.; Calabrese, V.; Cavazzini, M.; Pedron, D.; Cozzuol, M.; Licciardello, A.; Tuccitto, N.; Quici, S. *Dalton Trans.* **2008**, 2974−2982.
(21) Zaręba, J. K.; Białek, M. J.; Janczak, J.; Zoń, J.; Dobosz, A. *Cryst. Growth Des.* **2014**, *14*, 6143−6153.
(22) *CrysAlis CCD and CrysAlis Red program,* 171.31.8; Oxford Diffraction Poland: Wrocław, Poland, 2006.
(23) Sheldrick, G. M. *Acta Crystallogr., Sect. A: Found. Crystallogr.* **2008**, *64*, 112−122.
(24) Brandenburg, K.; Putz, K. *Diamond, Crystal and Molecular Structure Visualization,* Ver. 3.2i; University of Bonn: Bonn, Germany, 2012.
(25) Blatov, V. A.; Shevchenko, A. P.; Proserpio, D. M. *Cryst. Growth Des.* **2014**, *14*, 3576−3586.
(26) Spek, A. L. *J. Appl. Crystallogr.* **2003**, *36*, 7−13.
(27) Levesanos, N.; Grigoropoulos, A.; Raptopoulou, C. P.; Psycharis, V.; Kyritsis, P. *Inorg. Chem. Commun.* **2013**, *30*, 34−38.
(28) (a) Yao, M.-X.; Zeng, M.-H.; Zou, H.-H.; Zhou, Y.-L.; Liang, H. *Dalton Trans.* **2008**, 2428−2432. (b) Kapoor, P.; Pannu, A. P. S.; Hundal, G.; Kapoor, R.; Corbella, M.; Aliaga-Alcalde, N.; Hundal, M. S. *Dalton Trans.* **2010**, *39*, 7951−7959. (c) Singh Pannu, A. P.; Kapoor, P.; Hundal, G.; Kapoor, R.; Corbella, M.; Aliaga-Alcalde, N.; Singh Hundal, M. *Dalton Trans.* **2011**, *40*, 12560−12569. (d) Shurdha, E.; Moore, C. E.; Rheingold, A. L.; Miller, J. S. *Inorg. Chem.* **2011**, *50*, 10546−10548. (e) Maass, J. S.; Zeller, M.; Breault, T. M.; Bartlett, B. M.; Sakiyama, H.; Luck, R. L. *Inorg. Chem.* **2012**, *51*, 4903−4905.
(29) Zoń, J.; Videnova-Adrabinska, V.; Janczak, J.; Wilk, M.; Samoć, A.; Gancarz, R.; Samoć, M. *CrystEngComm* **2011**, *13*, 3474−3484.
(30) Liu, Y.; Xu, X.; Zheng, F.; Cui, Y. *Angew. Chem., Int. Ed.* **2008**, *47*, 4538−4541.

DOI: 10.1021/acs.inorgchem.5b01939
Inorg. Chem. 2015, 54, 10568−10575